Rare Metal Materials and Engineering
Volume 45, Issue 6, June 2016
Online English edition of the Chinese language journal

Available online at www.sciencedirect.com
ScienceDirect

Cite this article as: Rare Metal Materials and Engineering, 2016, 45(6): 1449-1454.

ARTICLE

Effect of Different Annealing Atmosphere on Ferroelectric Properties of 0.7$BiFeO_3$-0.3$PbTiO_3$ Thin Films

Li Haimin[1], Qiu Chunli[2], Zhu Jianguo[3], Huai Mingzhe[1], Yang Qingsong[1]

[1] Southwest Petroleum University, Chengdu 610500, China; [2] Sichuan Technology and Business College, Dujiangyan 611837, China; [3] Sichuan University, Chengdu 610064, China

Abstract: 0.7$BiFeO_3$-0.3$PbTiO_3$ (BFPT7030) thin films were deposited on $LaNiO_3/SiO_2/Si$ substrate by sol-gel process. The thin films were annealed in air, O_2 flow, air flow and N_2 flow in air environment by a rapid thermal annealing technique. Films annealed in air, O_2 flow and air flow were fully crystallized and showed highly (100) preferred orientation. BFPT7030 thin film annealed in N_2 flow could not obtain hysteresis loops because of the bad crystallization. The BFPT7030 thin films annealed in air showed the largest P_r of 30 μC cm^{-2} and the lowest leakage current density, while the film annealed in air flow showed the lowest P_r of 13 μC cm^{-2} and the largest leakage current. XPS results demonstrate that the Fe^{3+}:Fe^{2+} is 2.09:1, 1.65:1 and 1.5:1 for films annealed in air, O_2 flow and air flow, respectively, and the Bi and Pb relative content in the films annealed in O_2 flow and air flow is less than that of the film annealed in air. Fluctuation of Fe ions valence state and the volatilization of Bi are the main reasons for the generation of oxygen vacancies. Adding O_2 gas is helpful to prevent the generation of oxygen vacancies. Although volatilization of Pb would lead to inferior microstructure, no oxygen vacancies is generated during the process of volatilization of Pb.

Key words: annealing atmosphere; $BiFeO_3$-$PbTiO_3$; ferroelectric; sol-gel

$BiFeO_3$ has attracted much attention from perspectives of both fundamental physics and practical applications[1-4] because of its unique ferroelectric and antiferromagnetic ordering at room temperature[5-7]. $BiFeO_3$ has a very high Curie temperature of about 1100 K[8], which indicates that it possesses a high spontaneous polarization. Moreover, the first-principle study of spontaneous polarization in $BiFeO_3$ suggests that it has a large ferroelectric polarization of 90～100 μC·cm^{-2} [9]. However, both past and contemporary measurements showed much less polarization than predicated, especially in bulk form[10-14]. $BiFeO_3$ has a distorted perovskite structure which makes it unstable. To overcome this obstacle, the $BiFeO_3$-ABO_3 solid solution systems have attracted great attention as a solution for improved structural stability[15-17]. Among those perovskite ABO_3 compounds, $PbTiO_3$ is a stable ferroelectric perovskite oxide[18]. A (1-*x*)$BiFeO_3$-*x*$PbTiO_3$(BFPT100*x*) system is expected not only to provide the desired structural stabilization, but also exhibits a morphotropic phase boundary (MPB). According to the previous studies, the MPB of the BFPT100*x* system is located around the $x \approx 0.3$ composition, in which the tetragonal (*T*) and rhombohedral (*R*) phases coexist[19-22]. Although BFPT system showed relatively better structural properties. its ferroelectric polarization still exhibit not much high properties, Liu et al reported a remnant polarization (P_r) of 2.0 μC·cm^{-2} for BFPT100*x* (*x*=0.3) films prepared by a sol-gel method[23]. Sakamoto et al synthesized BFPT100*x* thin films by chemical deposition which showed a high ferroelectric polarization of 60 μC·cm^{-2}, but it was measured at –190 ℃[24]. Saturated *P-E* loops were not observed at room temperature due to the large leakage current in the high

Received date: June 24, 2015
Foundation item: Academic Level Pass of Southwest Petroleum University (201131010051); Set Sail Project of Southwest Petroleum University (2014QHZ022); Important Program of Education Department of Sichuan Province (14ZA0046)
Corresponding author: Zhu Jianguo, Ph. D., Professor, College of Materials Science and Engineering, Sichuan University, Chengdu 610064, P. R. China, Tel: 0086-28-85412415, E-mail: nic0400@scu.edu.cn

electric field.

BFPT-based thin films suffered from large leakage which is believed to result from oxygen vacancies arising from the hopping electrons from Fe^{3+} to Fe^{2+}. Oxygen vacancies act as a bridge between the Fe^{3+} to Fe^{2+} and leads to electron conduction[25]. And the volatilization of Pb and Bi, which leads to non-stoichiometry, would also increase the density of oxygen vacancies and increase the electron conduction. Since the leakage current of BFPT100*x* system mainly comes from oxygen vacancies and results in poor ferroelectric properties, this arouse our interest to assess the effect of annealing atmosphere (air, O_2 and N_2) on the ferroelectric properties. In the present paper, four $0.7BiFeO_3$-$0.3PbTiO_3$ (BFPT7030) thin films were deposited on $LaNiO_3/SiO_2/Si$ substrates via a sol-gel process by a rapid thermal technique (RTA). The as-deposited BFPT7030 thin films were annealed in air, O_2 flow, air flow and N_2 flow in the air environment. The microstructure and electric properties of these films were investigated The result analysis can be used as reference for preparing high quality BFPT100*x* thin films.

1 Experiment

BFPT7030 thin films were prepared on $LaNiO_3/SiO_2/Si$ substrates by a sol-gel process. The raw materials were bismuth nitrate pentahydrate [$Bi(NO_3)_3·5H_2O$], iron nitrate nonahydrate [$Fe(NO_3)_3·9H_2O$], lead acetate [$Pb(CH_3COO)_2·3H_2O$], and tetrabutyl titanate [$Ti(OC_4H_9)_4$].

Bismuth nitrate and iron nitrate were mixed with a mole ratio of 1:1 and incompletely dissolved in a small amount of acetic anhydride and acetic acid, then ethylene glycol was added, and stirred at room temperature for 3 h until bismuth nitrate and iron nitrate were completely dissolved. This solution was named solution A. Tetrabutyl titanate (stabilized by acetyl acetonate) was dissolved in ethylene glycol, stirred at 45 ℃ for 50 min; at the same time, lead acetate was dissolved at room temperature in ethylene glycol, stirred for 20 min and then added with diethanolanine, stirred for 30 min; then mixed tetrabutyl titanate solution and lead acetate solution, and stirred at 45 ℃ for 3 h. This solution was named solution B, lead acetate and tetrabutyl titanate were mixed with a mole ratio of 1:1. Finally solution B was mixed with solution A, and stirred at 45 ℃ for 16 h to form BFPT7030 sol. Diethanol amine was added to the final sol to increase the viscosity. The final concentration of lead acetate was 0.3 mol/L.

Four BFPT7030 thin films were prepared by depositing BFPT7030 sol for eight times. The films were annealed in air, O_2 flow, air flow and N_2 flow in the air environment. The depositions process was carried out by spin coating at 3000 r/min for 30 s in a super clean room. Each deposition layer was dried at 150 ℃ for 1 min and 200 ℃ for 3 min, followed by annealing at 700 ℃ for 90 s by rapid thermal annealing (RTA) technique with heating rate of 1 ℃ s^{-1}.

X-ray diffraction (XRD, DX-1000, Dandong, China) with Cu Kα radiation (λ=0.154 056 nm) in the mode of θ-2θ scan was used for the phase analysis of the films. The surface morphology of the BFPT7030 thin films was analyzed using a field emission-scanning electron microscope (FE-SEM, HITACHI S4800, Japan). The ferroelectric properties of the films were measured using Au as top electrodes, which were directly evaporated on the annealed films through a shadow mask with a diameter of 0.5 mm by DC sputtering, forming an $Au/BFPT/LNO/SiO_2/Si(100)$ stacked capacitor. The $LaNiO_3$ (LNO) layer of the $LaNiO_3/SiO_2/Si$ substrates was used as a bottom electrode. LNO was deposited on SiO_2/Si substrate by RF magnetron sputtering at the substrate temperature of 450 ℃ with the ratio of oxygen and argon of 10:40 SCCM (SCCM denotes cubic centimeter per minute at STP) under a working pressure of 2.0 Pa. The hysteresis loops of polarization (*P*) as a function of applied electric field (*E*) (*P*-*E* curve) and leakage current properties of the BFPT7030 thin films were evaluated by the Radiant Precision Ferroelectric Measurement System (RT2000 Tester, USA). X-ray photoelectron spectroscopy (XPS) were used to analyze Bi, Pb relative content and Fe oxidation state.

2 Results and Discussion

2.1 Microstructure of the BFPT7030 thin films

Fig.1 shows the XRD patterns of BFPT7030 thin films. All the films demonstrate a perovskite phase and fully crystallized except for the BFPT7030 films annealed in N_2 flow, which is quite different from other reports[26,27]. Very weak peaks are found in the BFPT7030 films annealed in N_2, indicating that the BFPT7030 thin films crystallize badly. This result may be attributed to the rapid thermal annealing (RTA) technique and the annealing temperature which is not much higher. The total time of heat treatment is less than 2 min, while in other literatures[26,27], the total time of the heat treatment of BFPT-based films is more than 1 h. Other films annealed in air and O_2 are completely crystallized and exhibit highly (100) preferred orientation. The preferential orientation parameter, α_{hkl}, can be calculated by the following formula:

$$\alpha_{hkl}=I_{hkl}/\sum I_{hkl} \quad (1)$$

where I_{hkl} is the relative intensity of the corresponding diffraction peak. The calculated preferential orientation α_{100} of the BFPT7030 thin films annealed in air, O_2 flow and air flow is 0.71, 0.77 and 0.75, respectively, indicating that BFPT7030 thin films are highly (100) oriented. Although the α_{100} of BFPT7030 thin film annealed in O_2 flow and air flow atmosphere is a little higher than that of the film annealed in air atmosphere, the peak height of BFPT7030 thin film annealed in O_2 flow and air flow atmosphere is much less than that of the film annealed in air, meaning that

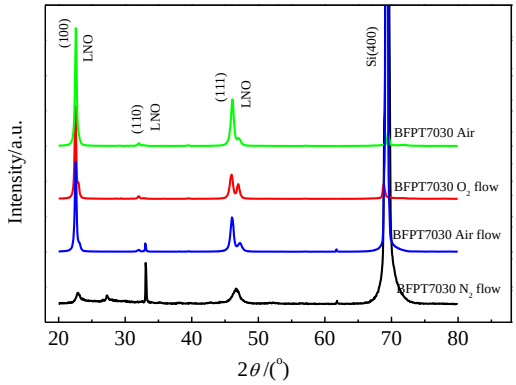

Fig.1 X-ray diffraction patterns for the films of BFPT7030 annealed in air, O_2 flow, air flow and N_2 flow at 700 ℃ by RTA

BFPT7030 thin film annealed in air has a better crystallization.

Fig.2 shows the surface and cross-section SEM images of BFPT7030 thin films annealed in air, O_2 flow, air flow and N_2 flow atmosphere. From these images, we can confirm that the BFPT7030 thin films are fully crystallized except for the film annealed in N_2 flow. Only a few crystalline grains are found in the film annealed in N_2, which means that BFPT7030 thin film annealed in N_2 atmosphere has an inferior crystallization and this is consistent with the XRD result. Grains of BFPT7030 thin film annealed in air, O_2 flow and air flow are fully grown up. From the four SEM surface images, we can see that the grain size of BFPT7030 thin film annealed in air is larger than that of films annealed in O_2 flow and air flow, indicating that BFPT7030 film annealed in air has a better crystallization than films annealed in O_2 flow and air flow, which is in consistent with the XRD results. Also we scanned the cross-section images of BFPT7030 thin films annealed in air and O_2 flow, as shown in Fig.2. BFPT7030 film annealed in O_2 flow exhibits more porous structures than that annealed in air, and the thickness is 754 nm and 774 nm for the films of BFPT7030 annealed in air and O_2, respectively. We ascribe this to the serious Bi and Pb volatilization in the O_2 and air flow atmosphere and thus it leads to worse crystallization and more porous structure than that of film annealed in air atmosphere.

And since BFPT7030 film annealed in N_2 flow crystallizes badly, we could not obtain its hysteresis loop and *I-V* curves. Thus we would not discuss the BFPT7030 film annealed in N_2 atmosphere in later part.

2.2 Ferroelectric properties of the BFPT7030 thin films

The ferroelectric hysteresis loops of these films measured at room temperature at a frequency of 500 Hz are shown in Fig.3. A saturated hysteresis loop was obtained in BFPT7030 thin film annealed in air, which shows the highest remnant polarization (P_r) of 30 μC·cm^{-2} with a coercive electric field (E_c) of 90 kV·cm^{-1}. However, BFPT7030 thin films annealed in O_2 flow and air flow show an unsaturated hysteresis loop and a lower P_r of 20 μC·cm^{-2} and 13 μC·cm^{-2} with a coercive electric field (E_c) of 90 kV·cm^{-1} and 92 kV·cm^{-1}, indicating that inferior ferroelectric properties are present in BFPT7030 thin films annealed in O_2 flow and air flow which results from higher electric conduction. And with higher electric conduction, BFPT7030 thin film annealed in O_2 flow and air flow can only endure the electric field as large as 200 kV·cm^{-1}, which is smaller than that of electric field of 270 kV·cm^{-1} for the film of BFPT7030 annealed in air.

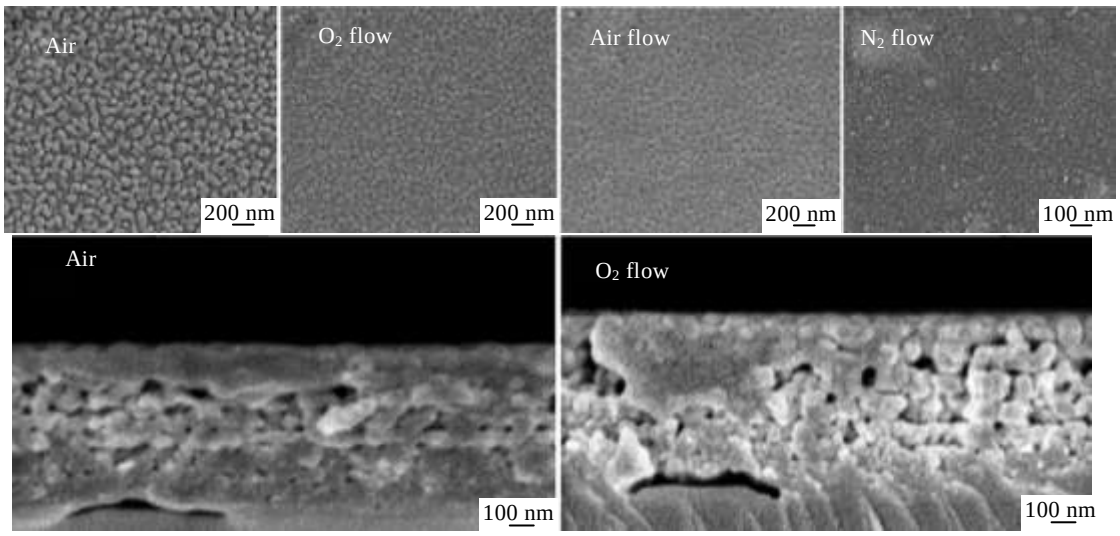

Fig.2 Surface SEM images of the BFPT7030 thin films annealed in air, O_2 flow, air flow and N_2 flow, and cross-section of BFPT7030 thin films annealed in air, and O_2 flow

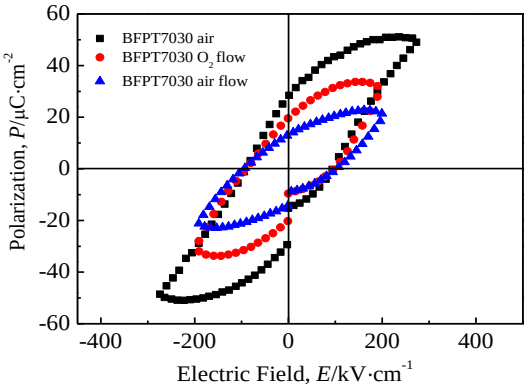

Fig.3 Ferroelectric *P-E* hysteresis loops measured at room temperature for the films of BFPT7030 annealed in air, O_2 flow and air flow

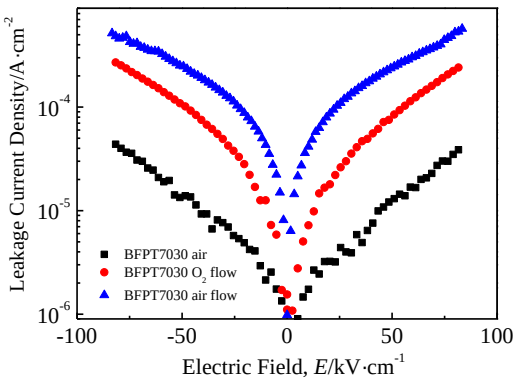

Fig.4 Leakage current density measured at room temperature for the films of BFPT7030 annealed in air, O_2 flow and air flow

2.3 Leakage current properties of the BFPT7030 thin films

The results of leakage current density as a function of electric field of BFPT7030 thin films annealed in air, O_2 flow and air flow measured at room temperature are shown in Fig.4. BFPT7030 thin films annealed in O_2 flow and air flow show obviously higher leakage current density in the whole electric field, indicating that flowing gas would lead to inferior insulation. BFPT7030 film annealed in O_2 flow shows better insulation than that of film annealed in air flow, indicating that more O_2 gas could prevent the generation of oxygen vacancies as predicted.

Since the BFPT7030 thin film annealed in flowing gas shows worse inferior ferroelectric properties and larger leakage current density than the film annealed in still air atmosphere, we considered that the main reason is the result of volatilization of Bi and Pb. Fig.5 shows the XPS results of Bi and Pb relative content for BFPT7030 films annealed in air, O_2 flow and air flow. From the diagram, it can be found that the content of Bi and Pb in BFPT7030 films annealed in O_2 flow and air flow are less than that of the film annealed in air, indicating that more Bi and Pb are volatilized. The chemical equation is as followed:

$$Bi^{3+}+O^{2-}\rightarrow Bi+(1/2)O_2+(1/2)Vo^{2+} \quad (2)$$

$$Pb^{2+}+O^{2-}\rightarrow Pb+(1/2)O_2 \quad (3)$$

Vo^{2+} represents the oxygen vacancies, which has two positive charges. From Eq.(3), it can be found that although Pb volatilizes, Eq. no oxygen vacancies are generated, which is mainly because the valence in both sides has to be equivalent. Only in reaction (2), generation of oxygen vacancies is accompanied by volatilization of Bi, and one Bi volatilizes, half one oxygen vacancy is generated. Thus, we can concludes that the volatilization of Bi would lead to non-stoichiometry and oxygen vacancies. At the same time, although volatilization of Pb would not lead to oxygen

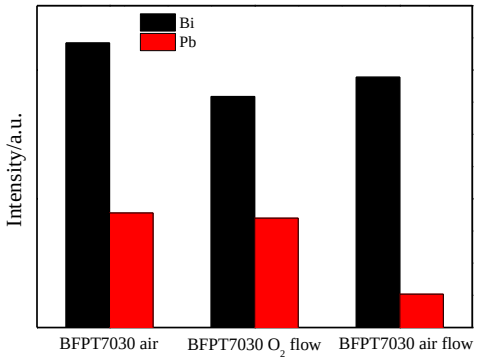

Fig.5 XPS results of Bi and Pb relative content for BFPT7030 films annealed in air, O_2 flow and air flow

vacancies, it would affect the microstructure of the thin films and thus leads to inferior ferroelectric properties. The BFPT7030 film annealed in O_2 flow shows better ferroelectric properties and lower leakage current than that of film annealed in air flow, indicating that O_2 gas could restrain the generation of oxygen vacancies.

The oxygen vacancies would not only came from the volatilization of Bi, but also came from the fluctuation of Fe ions valence state. The chemical equation is as followed:

$$4Fe^{3+}+O^{2-}\rightarrow 4Fe^{2+}+(1/2)O_2+Vo^{2+} \quad (4)$$

Fig.6 shows the XPS spectra of Fe $2p_{3/2}$ peak of BFPT7030 films annealed in air, O_2 flow and air flow. The Fe $2p_{3/2}$ peaks are split into two peak, 709.3 eV and 710.6 eV, corresponding to Fe^{2+} and Fe^{3+}, respectively [28,29]. From the peak area of Fe^{2+} and Fe^{3+}, it can be found that the content of Fe^{3+}:Fe^{2+} are 2.09:1, 1.65:1 and 1.5:1 for BFPT7030 films annealed in air, O_2 flow and air flow, manifesting that flowing gas would lead to more fluctuation of Fe ions valence state and generation of more oxygen

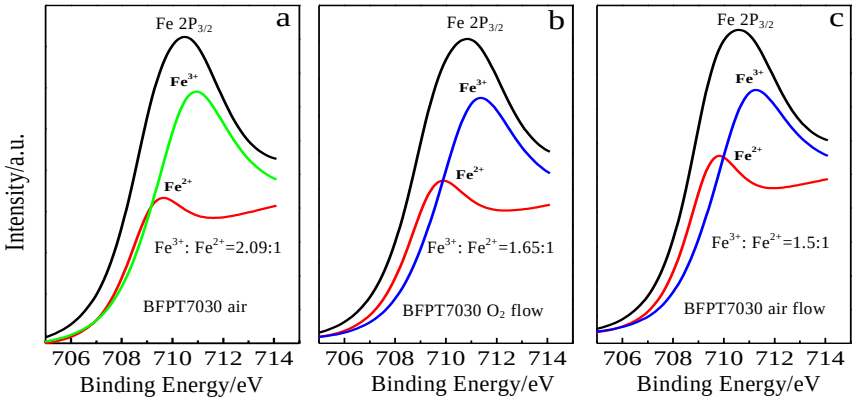

Fig.6 XPS spectra of Fe ions for BFPT7030 films annealed in air (a) O_2 flow (b) and air flow (c)

vacancies, as suggested by Eq.(4), while BFPT7030 film annealed in O_2 flow has a larger Fe^{3+}:Fe^{2+} than that of the film annealed in air flow, indicating that O_2 gas could prevent the generation of oxygen vacancies and the fluctuation of Fe ions valence state.

Thus, we can conclude that the inferior ferroelectric properties and large leakage current density result from the volatilization of Bi and fluctuation of Fe ions valance state, which would result in oxygen vacancies, and adding O_2 gas could prevent the generation of oxygen vacancies.

3 Conclusions

1) BFPT7030 thin films are deposited on $LaNiO_3/SiO_2/Si$ substrates by sol-gel process. The films are annealed in air, O_2 flow, air flow and N_2 flow in the air environment. XRD patterns show that BFPT7030 thin films are fully crystallized and highly (100) preferred orientation except for the film annealed in N_2 flow. Surface SEM images confirm that BFPT7030 thin film annealed in N_2 flow has a bad crystallization. No hysteresis loops or *I-V* curves are obtained in the BFPT7030 thin film annealed in N_2 flow because of the bad crystallization.

2) BFPT7030 thin films annealed in air show a saturated hysteresis loop with the highest P_r of 30 $\mu C \cdot cm^{-2}$ and a low E_c of 90 kV cm^{-1} measured at RT. While the BFPT7030 films annealed in O_2 flow and air flow exhibit unsaturated hysteresis loops and large leakage current density.

3) The large leakage current density comes from the fluctuation of Fe ions valence state and the volatilization of Bi. Oxygen vacancies are accompanied with the fluctuation of Fe ions valence state and the volatilization of Bi.

References

1 Seidel J, Martin L W, He Q *et al*. *Nature Materials*[J], 2009, 8: 229

2 Wang J, Neaton J B, Zheng H *et al*. *Science*[J], 2003, 299(5613): 1719

3 Shannigrahi S R, Huang A, Tripathy D *et al*. *Journal of Magnetism Magnetic Materials*[J], 2008, 320, 2215

4 Woo-Hee K, Sung M Y, Jong Y S *et al*. *Materials Letters*[J], 2014, 124: 47

5 Kubel F, Schmid H. *Acta Crystallographica B, Structural Science*[J], 1990, B46(6): 698

6 Sosnowska I, Peterlin-Neumaier T, Steichele E. *J Phys C: Solid State Phys*[J], 1982, 15: 4835

7 Fischer P, Polomaka M, Sosnowska I *et al*. *J Phys C: Solid State Phys*[J], 1980, 13: 1931

8 Kamba S, D. Nuzhnyy Savinov M *et al*. *Physical Review B*[J], 2007, 75: 024 403

9 Neaton J B, Ederer C, Waghmare U V *et al*. *Physical Review B*[J], 2005, 71: 014 113

10 Liu H R, Liu Z L, Yao K L. *J Sol-Gel Sci Techn*[J] 2007, 41: 123

11 Freitas V F, Cótica L F, Santos I A *et al*. *Journal of European Ceramic Society*[J], 2011, 31: 2965

12 Abe K, Sakai N, Takahashi J *et al*. *Japanese Journal of Applied Physics*[J], 2010, 49(9): 09

13 Huang D J, Deng H M, Yang P X *et al*. *Materials Letters*[J], 2010, 64: 2233

14 Liu Y T, Chen S Y, Li H Y. *Thin Solid Films*[J], 2010, 518: 7412

15 Singh S K, Shanthy S, Ishiwara H *et al*. *Journal of Applied Physics*[J], 2010, 108: 054 102

16 Ueda K, Tabata H, Kawai T. *Applied Physics Letters*[J], 1999, 75: 555

17 Chen L, Ren W, Zhu W *et al*. *Thin Solid Films*[J], 2010, 518: 1637

18 Tang Y L, Zhu Y L, Wang Y J *et al*. *Scientific Reports*[J], 2014, 4: 4115

19 Levin I, Krayzman V, Tucker M G *et al*. *Applied Physics Letters*[J], 2014, 104: 242 913

20 Amorín H, Correas C, Fernández-Posada C M *et al*. *Journal*

Applied Physics[J], 2014, 115: 104 104
21 Siddaramanna A, Kothai V, Srivastava C *et al*. *Journal of Physics D: Applied Physics*[J], 2014, 47: 045 004
22 Kothai V, Babu R Prasath, Ranjan R. *Journal of Applied Physical*[J], 2013, 114: 114 102
23 Liu H R, Liu Z L, Liu Q *et al*. *J Phys D: Appl Phys*[J], 2006, 39: 1022
24 Sakamoto W, Iwata A, Yogo T. *Journal of Applied Physics*[J], 2008, 104: 104 106
25 Zhu W M, Ye Z G. *Applied Physics Letters*[J], 2006, 89: 232904
26 Sakamoto W, Iwata A, Moriya M *et al*. *Materials Chemistry and Physics*[J], 2009, 116: 536
27 Singh V R, Dixit A, Garg A *et al*. *Applied Physics A*[J], 2008, 90: 197
28 Schedel-Niedrig Th, Weiss W, Schlögl R. *Physics Review B*[J], 1995, 52 (24): 17 449
29 Li H M, Guo H L, Li X D *et al*. *Journal of Inorganic Materials*[J], 2011, 26(10): 1053

不同退火气氛对 $0.7BiFeO_3$-$0.3PbTiO_3$ 薄膜铁电性能的影响

李海敏[1]，邱春丽[2]，朱建国[3]，淮明哲[1]，杨青松[1]
(1. 西南石油大学，四川 成都 610500)
(2. 四川工商职业技术学院，四川 都江堰 611837)
(3. 四川大学，四川 成都 610064)

摘　要：利用溶胶-凝胶法在$LaNiO_3/SiO_2/Si$衬底上制备了$0.7BiFeO_3$-$0.3PbTiO_3$（BFPT7030）薄膜，利用快速退火方式将薄膜分别在空气、氧气流、空气流、氮气流中进行后续退火处理。在空气、氧气流及空气流中退火的薄膜均完全结晶并呈现高度（100）择优取向。而在氮气流中退火的薄膜由于结晶很差，测试不出其电滞回线。空气中退火的BFPT7030薄膜表现出最大的剩余极化及最小的漏电流，P_r 为 30 μC·cm^{-2}, 而在空气流中退火的BFPT7030薄膜表现出最小的剩余极化(P_r: 13 μC·cm^{-2})及最大的漏电流。XPS测试结果表明，在空气、氧气流及空气流中退火的BFPT7030薄膜中Fe^{3+}:Fe^{2+}分别为2.09:1, 1.65:1 及 1.5:1。而在氧气流及空气流中退火的BFPT7030薄膜中Bi及Pb的相对含量低于在空气中退火的薄膜。铁离子的价态波动是产生氧空位的原因，增加氧气有助于抑制氧空位的产生。虽然Pb的挥发会导致较差的微观结构，但其挥发并不会导致氧空位的产生。

关键词：退火气氛；$BiFeO_3$-$PbTiO_3$；铁电；溶胶-凝胶

作者简介：李海敏，女，1978 年生，博士，讲师，西南石油大学材料科学与工程学院新能源材料及技术研究中心，四川 成都 610500，电话：028-83037409，E-mail: lucialee@126.com